RSC Advances

This article can be cited before page numbers have been issued, to do this please use: Y. Chen, Y. Lin, Y. Cheng and Y. J. Chang, *RSC Adv.*, 2015, DOI: 10.1039/C5RA17898C.

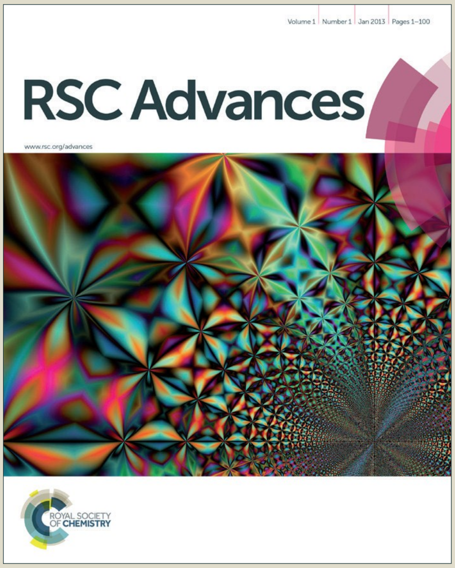

ROYAL SOCIETY
OF CHEMISTRY

www.rsc.org/advances

View Article Online
DOI: 10.1039/C5RA17898C

Synthesis of Novel Isophorone-based Dyes for Dye-sensitized Solar Cells

Yih-Chun Chen, Yan-Zuo Lin, Yu-Ting Cheng, and Yuan Jay Chang*

Received (in XXX, XXX) Xth XXXXXXXXX 20XX, Accepted Xth XXXXXXXXX 20XX
DOI: 10.1039/b000000x

Four organic dyes containing isophorone as the π-bridge unit were synthesised, their photophysical and electrochemical properties were characterised, and they were then used for fabricating dye-sensitised solar cells (DSSCs). Arylamine derivatives and cyanoacrylic acid functioned as an electron donor (D) and acceptor (A), respectively, to form a D–π–A system by using lack of a Pd-catalysed process. **YC-1** exhibited a hexyloxy long chain and strong phenothiazine donor moiety, improved both the open-circuit voltage (V_{oc}) and short-circuit current (J_{sc}), and reduced charge recombination. The optimal device exhibited a J_{sc} of 14.86 mA·cm^{-2}, a V_{oc} of 0.67 V, a fill factor of 0.62, and a photon-to-current conversion efficiency of 60% at 385–605 nm, corresponding to an overall conversion efficiency of 6.18%. The photophysical properties of the DSSCs were analysed using a time-dependent density functional theory model with the B3LYP functional. The electronic nature of the devices was elucidated using electrochemical impedance spectroscopy (EIS) and controlled intensity modulated photo spectroscopy (CIMPS).

1. Introduction

The global problems of the limited supply of fossil fuels and CO_2 emission has prompted the investigation and development of renewable and environment-friendly energy sources. In general, solar energy is widely acknowledged as a potential alternative energy resource. Compared with silicon-based photovoltaic devices, dye-sensitized solar cells (DSSCs) have received considerable attention because they are easy to fabricate, have a wide absorption range because of the tuning structure, are colourful and transparent, and have a low cost.[1] O'Regan and Grätzel have reported that DSSCs utilizing ruthenium-based complexes, namely **N3**, **N719**, black dye, and **Z907**, yield a high power conversion efficiency of >11%.[2] Furthermore, Diau et al. used a porphyrin dye and achieved a maximal performance of 13%.[3] However, a previous report on a metal-complex sensitizer reported a complicated synthetic route, difficult purification, and a low yield. The photosensitizer is the most crucial factor determining the performance of DSSCs, and numerous metal-free organic dyes have been investigated and exhibited high performance, similar to that of **N719** in DSSCs.[4] Metal-free organic dyes are environment friendly, have a low cost and high structural flexibility, and can be easily prepared; most of these organic dyes have linearly shaped molecules, comprising a strong dipole, an electron donor (D), a π-bridge, an electron acceptor (A), and a D–π–A system. For achieving an optimal D–π–A system for DSSCs, it is critical to improve the short-circuit current (J_{sc}) and open-current voltage (V_{oc}).

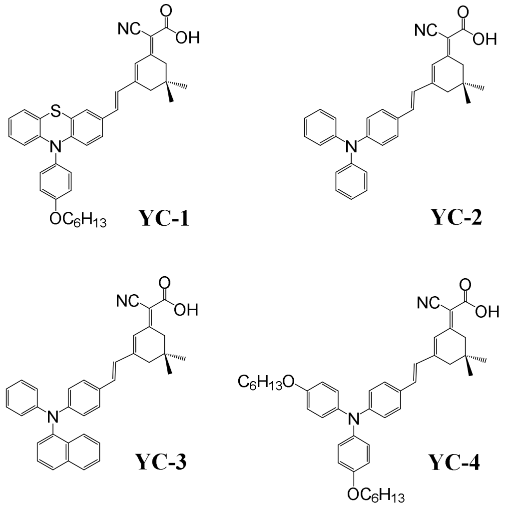

Fig.1 Organic dye structures of **YC**-series.

In general, the π-bridge unit in the sensitizer is mainly composed of thiophene,[5] furan,[6] pyrrole,[7] benzene,[8] diketopyrrolopyrrole,[9] and benzothiadiazole[10] as linkers. However, most of the C–C bond is formed for connecting bridges to the donor or acceptor moiety of sensitizers by Pd catalysed through cascade reactions, such as Sonogashira, Heck, Suzuki–Miyaura, and Stille coupling reactions. Although a Pd-based cross-coupling reaction is a more powerful method for linking two moieties through a simple, time-efficient, and versatile synthesis route, Pd is costly and not environment friendly.

Data on the use of the low-cost isophorone with a simple structure as the π-bridge for DSSCs are rare. Sugihara and Tian *et al*. reported high efficiencies of **NKX-2753** and **D-3** that incorporated coumarin and indoline derivatives, respectively, as donor groups.[11,12] In this study, we modified and designed four **YC**-series dyes by using isophorone as the π-bridge between the arylaimine electron donor and cyanoacrylic acid acceptor without using a Pd-catalysed procedure. In a previous study, we reported

---

Department of Chemistry, Tung Hai University, Taichung 407, Taiwan. E-mail: jaychang@thu.edu.tw; Fax:+886-4-23590426; Tel: +886-4-23590121 ext 32224

† Electronic Supplementary Information (ESI) available: Experimental data of compound **B**~**D**, the ^{1}H and ^{13}C NMR spectra, theroetical calculation, UV/vis spectra, CV spectra, EIS spectra, and the devices incooperating DCA. See DOI: 10.1039/b000000x/

View Article Online
DOI: 10.1039/C5RA17898C

phenothiazine, which possesses electron-rich nitrogen and sulphur heteroatoms, with its molecular structure exhibiting a slight bend in the central ring.[13] A long chain increases solubility and reduces the dark current by covering the TiO_2 surface.[4h, 14] In this study, we investigated whether the introduction of arylamine (**YC-4**) or phenothiazine (**YC-1**) with long alkoxy chains into DSSCs enhances the light-harvesting function and $V_{\rm oc}$; **YC-2** and **YC-3** served as references. The synthetic procedures are described in Scheme 1, and all structures were confirmed according to their spectroscopic data.

2. Experimental

Characterization and reagents

All reactions and manipulations were conducted under a nitrogen atmosphere, and solvents were freshly distilled according to standard procedures. ^{1}H and ^{13}C nuclear magnetic resonance (NMR) spectra were recorded on Bruker (AV 300/AV400/AVIII HD 400/AV 500 MHz) spectrometers in $CDCl_3$ as the solvent. Chemical shifts (δ) were reported downfield from the peak with respect to tetramethylsilane. The absorption spectra were recorded on a Shimadzu UV-1800 spectrophotometer, and the emission spectra and photo-luminescence quantum yield were obtained from a Hitachi F-4500 spectrofluorometer. The redox potentials were measured by using cyclic voltammetry on a CHI 620 analyser. All measurements were conducted in tetrahydrofuran solutions containing 0.1 M tetrabutylammonium hexaflourophosphate as the supporting electrolyte under ambient conditions after purging for 10 minutes with N_2. Furthermore, the conventional three-electrode configuration was employed, comprising a glassy carbon working electrode, a platinum counter electrode, and an Ag/Ag$^+$ reference electrode calibrated using ferrocene/-ferrocenium as an internal reference. Mass spectra were recorded using a JEOL JMS-700 double-focusing mass spectrometer. Ethyl 2-cyanoacetate, ammonium acetate, benzene, n-butyllithium (1.6 M in hexane), N,N-dimethylformamide, piperidine, lithium hydroxide (LiOH), acetic anhydride, and acetonitrile (MeCN) were separately purchased from ACROS, Alfa, Merck, Lancaster, TCI, Sigma–Aldrich, and Showa. Chromatographic separations were performed using precoated silica gel plates (Kieselgel si 60, 40–63 µm; Merck).

Fabrication and Characterization of DSSCs.

Fluorine-doped tin oxide (FTO) conducting glass (FTO glass, Solaronix TCO22-7; sheet resistance, 7 Ω square^{-1}) and Ti-Nanoxide T/SP and Ti-Nanoxide R/SP titania-oxide pastes were purchased from Solaronix. A thin film of TiO_2 (10–12 µm transparent + 5 µm scattering) was coated on a 0.25 cm^2 FTO glass substrate, which was then immersed in a THF or CH_2Cl_2 solution containing 3×10^{-4} M dye sensitisers for 12 h, rinsed with anhydrous acetonitrile, and dried. Another piece of FTO glass with a 100 nm thick layer of sputtered Pt was used as a counter electrode. The active area was controlled at a dimension of 0.25 cm^2 by adhering a 60 µm thick piece of polyester tape to the Pt electrode. The photocathode was placed on the top of the counter electrode and was tightly clipped to form a cell, and an electrolyte was injected into the seam between the two electrodes. An acetonitrile solution containing LiI (0.5 M), I_2 (0.05 M), and 4-*tert*-butylpyridine (TBP; 0.5 M) was used as electrolyte 1 (E1). A solution of 3-dimethylimidazolium iodide (1.0 M), LiI (0.05 M), I_2 (0.03 M), guanidinium thiocyanate (0.1 M), and TBP (0.5 M) in MeCN:valeronitrile (85:15, v/v) was used as electrolyte 2 (E2). Devices composed of the commercial dye N719 under the same conditions (3×10^{-4} M, Solaronix S.A., Switzerland) were used as references. The cell parameters were obtained under incident light that had an intensity of 100 mW·cm^{-2} measured using a thermopile probe (Oriel 71964), was generated by a 300 W solar simulator (Oriel Sol3A Class AAA Solar Simulator 9043A, Newport), and passed through an AM 1.5 filter (Oriel 74110). The light intensity was further calibrated using an Oriel reference solar cell (Oriel 91150) and adjusted to 1.0 sun. Moreover, the monochromatic quantum efficiency was recorded using a monochromator (Oriel 74100) under a short circuit condition. Electrochemical impedance spectra of DSSCs were recorded by an Impedance/CEM/IVMS analyzer (Zahner Ennium).

(E,Z)-2-Cyano-2-(3-((E)-2-(10-(4-(hexyloxy)phenyl)-10H-phenothiazin-3-yl)vinyl)-5,5-dimethylcyclohex-2-en-1-ylidene)acetic acid (YC-1). Compounds **E-1** (5 g, 18.3 mmol) and 2 M LiOH were placed in a one-necked flask by using ethanol, water, and THF and heated to 50 °C for 3 h. The reaction was neutralised by adding 1 M HCl at room temperature, and the product was extracted using DCM. The organic layer was dried over anhydrous $MgSO_4$ and evaporated under vacuum. The product was then purified using silica gel column chromatograph with methylene chloride as the eluent. A red solid (**YC-1**) was obtained in an 83% yield. $\delta_{\rm H}$ (500 MHz, $CDCl_3$) 7.27 (s, 1H), 7.26 (s, 1H), 7.10–7.13 (m, 3H), 6.90–6.97 (m, 3H), 6.81–6.83 (m, 4H), 4.04 (t, 2H, J = 6.15 Hz), 2.96 (s, 1H), 2.65 (s, 1H), 2.39 (s, 1H), 2.37 (s, 1H), 1.82–1.87 (m, 2H), 1.52–1.54 (m, 2H), 1.35–1.38 (m, 4H), 1.03–1.06 (m, 6H), 0.93 (t, 3H, J = 6.3 Hz). $\delta_{\rm C}$ (125 MHz, $CDCl_3$) 168.8, 167.1, 166.5, 159.0, 154.0, 153.6, 145.4, 143.6, 134.5, 132.4, 131.8, 130.2, 130.1, 128.3, 127.6, 126.9, 126.8, 126.5, 125.9, 125.2, 124.9, 123.8, 122.7, 120.0, 118.9, 117.1, 116.5, 116.3, 115.9, 115.6, 97.6, 96.8, 68.3, 44.9, 41.1, 39.2, 38.8, 31.9, 31.6, 31.5, 29.2, 28.3, 28.1, 25.7, 22.6, 14.0. MS (FAB, 70 eV): m/z (relative intensity) 590 (M$^+$, 100); HRMS calcd for $C_{37}H_{38}N_2O_3S$: 590.2603, found 590.2597.

(*E*,*Z*)-2-Cyano-2-(3-((*E*)-4-(diphenylamino)styryl)-5,5-dimethylcyclohex-2-en-1-ylidene)acetic acid (YC-2). Compound **YC-2** was synthesised using the procedure used for **YC-1**. A red solid (**YC-2**) was obtained in an 87% yield. $\delta_{\rm H}$ (400 MHz, $CDCl_3$) 7.90 (s, 0.5H), 7.39 (d, 1H, J = 8.6 Hz), 7.38 (d, 1H, J = 8.6 Hz), 7.29–7.33 (m, 4H), 7.08–7.16 (m, 6.5H), 7.00–7.05 (m, 2H), 6.90–6.97 (m, 2H), 3.00 (s, 1H), 2.69 (s, 1H), 2.46 (s, 1H), 2.44 (s, 1H), 1.10 (s, 3H), 1.07 (s, 3H). $\delta_{\rm C}$ (100 MHz, $CDCl_3$) 169.0, 168.0, 167.4, 167.3, 154.3, 154.0, 149.2, 149.1, 146.9, 135.7, 135.6, 129.4, 129.3, 129.2, 128.5, 128.3, 127.6, 125.7, 125.3, 125.2, 123.9, 123.8, 123.7, 122.2, 122.1, 117.1, 116.4, 97.5, 96.7, 45.0, 41.2, 39.3, 38.9, 31.9, 31.5, 28.3, 28.1. MS (FAB, 70 eV): m/z (relative intensity) 460 (M$^+$, 100); HRMS calcd for $C_{31}H_{28}N_2O_2$: 460.2151, found 460.2149.

View Article Online
DOI: 10.1039/C5RA17898C

(*E*,*Z*)-2-cyano-2-(5,5-dimethyl-3-((*E*)-4-(naphthalen-1-yl-(phenyl)amino)styryl)cyclohex-2-en-1-ylidene)acetic acid (YC-3). YC-3 was synthesised using the procedure used for **YC-1**. A red solid (**YC-3)** was obtained in an 85% yield. δ_H (400 MHz, CDCl$_3$) 7.91 (t, 2H, J = 8.2 Hz), 7.87 (s, 0.5H), 7.83 (d, 1H, J = 8.2 Hz), 7.47–7.53 (m, 2H), 7.32–7.41 (m, 4H), 7.25–7.29 (m, 2H), 7.14–7.17 (m, 2H), 7.02–7.07 (m, 2H), 6.87–6.94 (m, 4.5H), 2.99 (s, 1H), 2.68 (s, 1H), 2.43 (s, 1H), 2.42 (s, 1H), 1.08 (s, 3H), 1.06 (s, 3H). δ_C (100 MHz, CDCl$_3$) 154.4, 154.0, 149.8, 149.7, 147.2, 142.6, 135.9, 135.8, 135.3, 131.1, 130.0, 129.3, 129.2, 128.6, 128.5, 128.3, 127.9, 127.4, 127.2, 127.1, 126.6, 126.3, 125.5, 123.9, 123.5, 123.4, 123.3, 123.2, 120.2, 120.1, 117.1, 116.4, 97.3, 96.5, 45.0, 41.2, 39.3, 38.9, 31.9, 31.5, 28.3, 28.1. MS (FAB, 70 eV): m/z (relative intensity) 510 (M$^+$, 100); HRMS calcd for $C_{35}H_{30}N_2O_2$: 510.2302, found 510.2291.

***(E,Z)-2-(3-((E)-4-(bis(4-(hexyloxy)phenyl)amino)styryl)-5,5-dimethylcyclohex-2-en-1-ylidene)-2-cyanoacetic acid* (YC-4).** Compound **YC-4** was synthesised using the procedure used for **YC-1**. A red solid (**YC-4)** was obtained in an 87% yield. δ_H (400 MHz, CDCl$_3$) 7.89 (s, 0.5H), 7.28–7.33 (m, 2H), 7.01–7.10 (m, 4H), 6.85–6.94 (m, 8.5H), 3.94–3.98 (m, 4H), 3.00 (s, 1H), 2.67 (s, 1H), 2.43 (s, 1H), 2.41 (s, 1H), 1.76–1.82 (m, 4H), 1.47–1.50 (m, 4H), 1.36–1.38 (m, 8H), 1.08 (s, 3H), 1.06 (s, 3H), 0.94 (t, 6H, J = 6.52 Hz). δ_C (100 MHz, CDCl$_3$) 168.7, 168.0, 166.9, 156.2, 156.1, 154.5, 154.1, 150.1, 150.0, 139.7, 139.6, 136.0, 135.9, 128.6, 127.4, 127.3, 127.2, 126.6, 125.3, 123.3, 119.1, 119.0, 117.5, 116.7, 115.4, 97.5, 96.6, 68.2, 45.0, 41.2, 39.3, 38.9, 31.9, 31.6, 31.5, 29.3, 28.3, 28.1, 25.7, 22.6, 14.0. MS (FAB, 70 eV): m/z (relative intensity) 660 (M$^+$, 100); HRMS calcd for $C_{43}H_{52}N_2O_4$: 660.3922, found 660.3916.

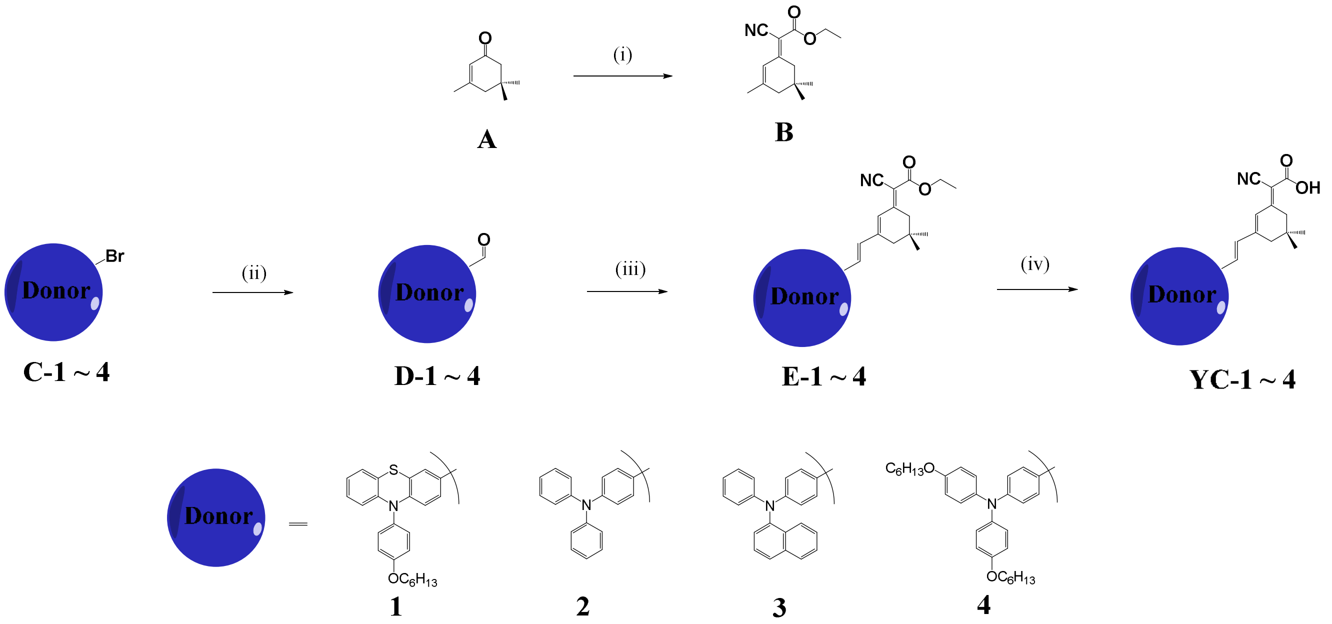

Scheme 1. Synthetic route of organic dyes. Reagents and conditions: (i) Ethyl 2-cyanoacetate, NH$_4$OAc, benzene, acetic anhydride, reflux; (ii) *n*-BuLi, DMF, THF, -78 ℃; (iii) compound **2** , piperidine, CH$_3$CN, 90 °C; (iv) LiOH, EtOH/ H$_2$O/ THF, 50 ℃.

Quantum Chemistry Computations

The structures of dyes were optimized using the B3LYP/6-31G* hybrid functional. For the excited states, a time-dependent density functional theory (TDDFT) with the B3LYP functional was employed. All analyses were performed using the Q-Chem 3.0 software. The frontier orbital plots of the highest and lowest occupied molecular orbitals (hereafter referred to as the HOMO and LUMO, respectively) were drawn using GaussView 04.

Results and discussion

Synthesis

The structures of the dyes are shown in Fig. 1, and their synthetic sequences are outlined in Scheme 1. The **YC** series contained an isophorone moiety as the bridge unit in the sensitizer. Its synthesis started with isophorone yielding an ester unit of **B** (*E*/*Z*: 1/1) through Knoevenagel condensation, and the isomer ratio was verified using proton NMR (Fig. S1).[12] A bromo group was replaced with aldehyde on the donor moiety of **D-1~4** by n-butyllithium and DMF. The donor part was then connected to the π-bridge and acceptor part by using the Knoevenagel condensation reaction to yield **E-1~4**. Four final products were obtained in high yields and easily purified through base hydrolysis of an ester to construct the cyanoacrylic acid acceptor unit. The structures of all new compounds were characterised

View Article Online
DOI: 10.1039/C5RA17898C

according to their spectroscopic data.

Absorption spectra

The ultraviolet–visible absorption spectra of all dyes in the CH_2Cl_2 solution and on TiO_2 are shown in Figs. 2 and 3, and the parameters are listed in Table 1. All sensitizers exhibit broad and high intensity absorption in the range 344–504 nm. The short wavelength region at 344–370 nm is attributed to localized π–π* transitions, whereas the long wavelength region in the range of 476–504 nm is attributed to intramolecular charge-transfer transition (ICT). Compared with the other three compounds, the intensity of the π–π* transition of **YC-1** was stronger with the phenothiazine donor moiety, indicating that the phenothiazine donor highly enhances π-overlapping compared with the fan structure of triphenylamine. Furthermore, **YC-1** and **YC-4** exhibited more broadened and high-intensity ICT transitions because the alkoxy chain improved not only the donating ability of the donor moiety but also the coplanar conformation of the bridge moiety between the donor and acceptor. A slightly different optimized structure was evidenced by theoretical computation according to the TDDFT with the B3LYP functional in combination with the standard 6-31G* basis set (Fig. 5). The phenomenon was consistent with the dipole moments revealed by computation results (Table S1). The absorption photocurrent (J_{sc}) in the area and intensity of absorption exhibit the same trend in solutions.

The absorption spectra of all dyes absorbed on the TiO_2 surface are shown in Fig. 3. Compared with the absorption spectra of **YC-2** and **YC-3**, those of **YC-1** and **YC-4** are broader, representing an advantageous spectral property for light harvesting. All dyes exhibited a blue-shift of approximately 55–71 nm in the film ICT absorption band with respect to those in solutions, and the spectral difference among all dyes diminished. The blue-shift, a common phenomenon for most organic dyes, appears to be a result of deprotonation of the carboxylic acid or strong interaction between the dye and semiconductor surface when it is anchored onto the TiO_2 surface.

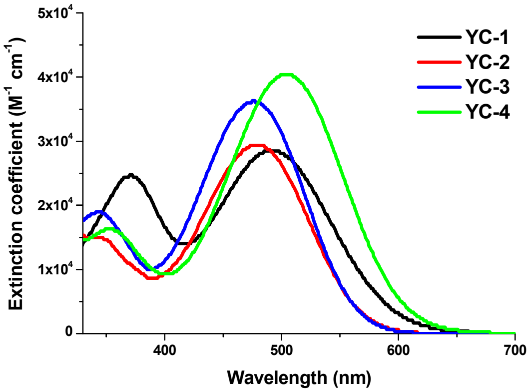

Fig. 2 Absorption spectra of dyes in CH_2Cl_2 solution.

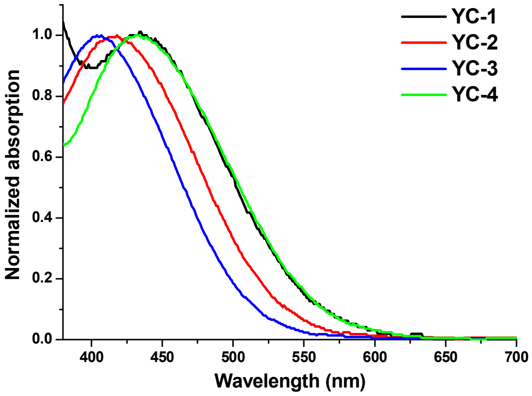

Fig. 3 Normalized absorption spectra of YC-series organic dyes on TiO_2.

Electrochemical Properties

The oxidation potentials (E_{ox}), corresponding to the HOMO level of the dyes, were measured using cyclic voltammetry. It is clear that the long hexyloxy chain in the arylamine donor moiety effectively influences the electron delocalization and oxidation potential. The lowest ionization potentials in CH_2Cl_2 solutions decreased in the order of **YC-2** ≈ **YC-3** > **YC-4** ≈ **YC-1** (Fig. 4 and S19). Moreover, the LUMO levels of the dyes were estimated according to the E_{ox} values and the zero–zero band gaps at the onset of the absorption spectra (Table 1). **YC-1** and **YC-4** possess a narrower HOMO–LUMO energy gap, consistent with the wider absorption ranges in Fig. 2. This observation was confirmed by theoretical calculations, as discussed in the following section. For the appropriate functioning of DSSCs, all sensitizers were maintained more positive than the redox potential of the iodine/iodide electrolyte (0.4 V vs. the normal hydrogen electrode, NHE), ensuring a sufficient driving force for regenerating the oxidized dyes from the electrolytes. The LUMO levels of all sensitizers were higher than the conduction bands (−0.5 V vs. NHE) of TiO_2. The energy levels of all dyes are in accordance with the requirements for efficient electron flow.

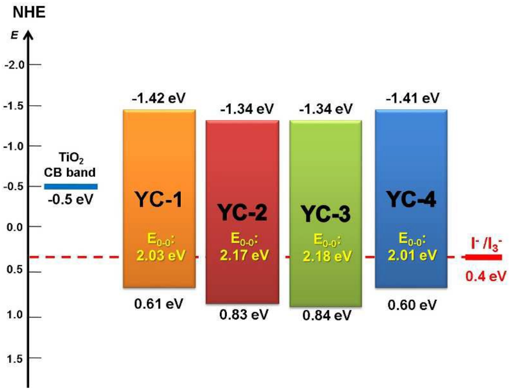

Fig. 4 HOMO - LUMO energy levels of the **YC**-series sensitizer.

View Article Online
DOI: 10.1039/C5RA17898C

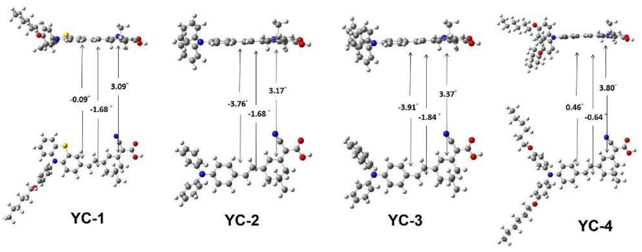

Fig. 5 Optimized structure of **YC**-series organic dyes estimated by time-dependent DFT/B3LYP (6-31G* basis set).

Computational analysis

The effects on device performances of **YC-1–4** were further explored through theoretical models. Complete geometrical optimizations were performed using the B3LYP/6-31G* hybrid functional implanted in Q-Chem 3.0.[16] The optimized molecular geometry of **YC-1–4** is depicted in Fig. 5 and shows that the conformation of the isophorone bridge unit is nearly coplanar; however, the orientation of the dimethyl group on the isophorone ring that appears slightly bulky prevents intramolecular aggregation. The electron distributions of frontier orbitals are shown in Fig. S17,† and as depicted, the electron densities in the HOMOs were mainly distributed around the amine donor moieties and those in the LUMOs around the cyanoacrylic acid of the acceptor moieties. A delicate balance between charge separation and recombination must be maintained by modifying the molecular structures. As per our review of relevant literature, a disturbance to π-conjugation, either a distortion of the molecular geometry or an interruption of the intramolecular aggregation by a long chain, may reduce the charge migration rate. As long as the charge-separated state can maintain a longer lifetime, a higher device quantum efficiency can be achieved.[17] A difference in Mulliken charge distributions between the ground state (S_0) and excited state (S_1) is plotted according to the estimate generated using the time-dependent DFT/B3LYP model in Fig. 6 and Table S2.† **YC-1** and **YC-4** exhibited optimal charge separation in the ICT state (bar chart, Fig. 6). In brief, both compounds exhibited a slightly higher V_{oc} value than did **YC-2** and **YC-3** in DSSCs with E1.

Photoexcitation pumps an electron from the HOMO to LUMO and therefore shifts a considerable amount of electrons from the donor to acceptor. Consequently, the HOMO–LUMO energy gap in **YC-1** and **YC-4** is lower than in that in **YC-2** and **YC-3;** therefore, the ICT band in the former exhibited a bathochromic shift with respect to the latter. It also comprises the dipole moment (**YC-1**: 12.8343 D; **YC-4**: 11.9272 D) and zero–zero energy of **YC**-series sensitizers.

The transition probability was estimated according to excitation by using the time-dependent DFT/B3LYP model, and the calculated oscillator strength (*f*) is shown in Table S1.† The *f* values for the lowest energy transitions of the ICT transitions (S1 state) are all relatively high, ranging from 0.61 to 1.13. The results are consistent with the absorptivity measured in solutions.

Photovoltaic performance of DSSCs

DSSC devices composed of the synthesised dyes were fabricated on the surface of TiO_2 according to a standard procedure.

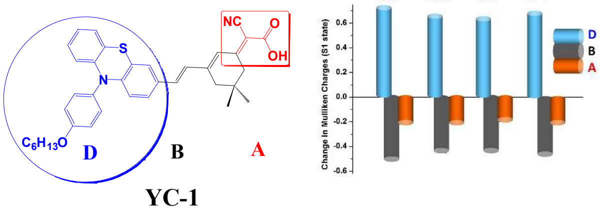

Fig. 6 Difference of Mulliken charges between ground state (S_0) and excited state (S_1), estimated by time dependent DFT/B3LYP model.

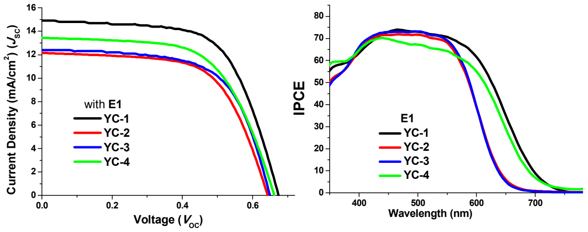

Fig. 7 *J-V* plots and IPCE of DSSCs devices of **YC-1~4** with E1 electrolyte. The plots were measured under the light intensity of 1.0 sun.

Two types of electrolytes were used for investigating the performance of devices: E1 was composed of LiI (0.5 M), I_2 (0.05 M), and TBP (0.5 M) in MeCN, whereas E2 was composed of 3-dimethylimidazolium iodide (1.0 M) and guanidinium thiocyanate (0.1 M) in addition to LiI (0.05 M), I_2 (0.03 M), and TBP (0.5 M) in a mixed solvent of MeCN and valeronitrile (85:15, v/v). Experiments involving co-absorption by using deoxycholic acid (DCA) were conducted. The incident photocurrent conversion efficiencies (IPCEs) and photocurrent–voltage (*J–V*) curves of all dyes were measured under AM 1.5 solar light (100 mW·cm^{-2}); the short circuit current (J_{sc}), open circuit voltage (V_{oc}), fill factor (FF), and solar-to-electrical photocurrent density (η) are summarised in Table 1, where **N719** serves as a reference dye.

The *J–V* plots and IPCEs of all devices with E1 are shown in Fig. 7. The apparent improvement of the V_{oc} values was observed using E2; specifically the values were approximately 0.02–0.05 V higher than those obtained using E1 (Table 1). The varieties interaction in different solvents might cause diversity of the chemical and physical properties between the sensitizer and TiO_2 surface.[18] Two types of solvents were used: THF and CH_2Cl_2. The devices fabricated using CH_2Cl_2 exhibited the optimal result (Tables S3). Therefore, the parameters of all **YC**-series dyes listed in Tables 1 and 2 are those of devices with the CH_2Cl_2 solvent system.

An apparent improvement in the V_{oc} values was observed using E2; specifically, the values were approximately 0.02–0.07 V higher those obtained using E1. Furthermore, the lower concentration of Li ions in E2 raised the Fermi energy level of the conduction band of TiO_2, enhancing the V_{oc} values and subsequently increasing the gap between the conduction band of TiO_2 and E2.[19] Although the V_{oc} values of all devices with E2 were considerably higher than those with E1, the J_{sc} values were

View Article Online
DOI: 10.1039/C5RA17898C

considerably lower, particularly that of **YC-2** (approximately 17%), as Table 1 shows.

Table 1 Photochemical and electrochemical parameters of the dyes.

dye	$\lambda_{max}{}^{a}$ (nm)/ ε ($M^{-1}cm^{-1}$)	λ_{max} (TiO_2)	$E_{ox}{}^{b}$ (V)	$E_{0\text{-}0}$ (eV)	$E_{red}{}^{c}$ (V)	J_{sc} ($mA{\cdot}cm^{-2}$) E1/E2^{e}	V_{oc} (V) E1/E2	FF E1/E2	η^{d} (%) E1/E2	Loading amount (10^{-7}mol/cm^{-2})
YC-1	491 (28500)	436	0.61	2.03	-1.42	14.86/11.91	0.67/0.69	0.62/0.63	6.18/5.17	13.4
YC-2	478 (29300)	416	0.83	2.17	-1.34	12.18/10.15	0.64/0.71	0.63/0.64	4.92/4.61	6.3
YC-3	476 (36300)	405	0.84	2.18	-1.34	12.43/10.78	0.65/0.67	0.63/0.61	5.08/4.43	8.3
YC-4	504 (40300)	434	0.60	2.01	-1.41	13.44/12.42	0.66/0.69	0.60/0.61	5.37/5.20	11.8
N719	—	—	1.10^{f}	2.60^{f}	-1.50^{f}	16.22/16.32	0.73/0.75	0.59/0.60	7.02/7.34	—

[a] Absorption and Emission are in CH_2Cl_2. [b] Oxidation potential in THF (10^{-3} M) containing 0.1 M $(n\text{-}C_4H_9)_4NPF_6$ with a scan rate 50 mV·s^{-1} (*vs.* NHE). [c] E_{red} calculated by $E_{ox} - E_{0\text{-}0}$. [d] Performance of DSSCs measured in a 0.25 cm^2 working area on a FTO (7 Ω/square) substrate. [e] Electrolyte 1 (E1): LiI (0.5 M), I_2 (0.05 M), and TBP (0.5 M) in MeCN. Electrolyte 2 (E2): 3-dimethylimidazolium iodide (1.0 M), LiI (0.05 M), I_2 (0.03 M), guanidinium thiocyanate (0.1 M), and TBP (0.5 M) in MeCN:valeronitrile (85:15, v/v). [f] see reference 20.

The long hexyloxy chains of **YC-1** and **YC-4** may prevent contact between I_3^- and the surface of TiO_2, and these compounds exhibited higher V_{oc} values than those of the other two sensitisers, which had no long chain.[4c, 4j, 21] Therefore, **YC-1** and **YC-4** can reduce the dark current by lowering the rate of charge recombination more substantially than **YC-2** and **YC-3** do.

The alignment of dyes on the surface of TiO_2 is a crucial factor for further optimising the performance of DSSCs. The sensitiser must be carefully planted vertically on TiO_2 for preventing intermolecular aggregation in dark current. Whether adding a DCA coabsorbent prevents dye lying on the TiO_2 surface was examined. For some dyes unable to form high quality films, adding DCA can effectively improve the film morphology and consequently reduce the charge recombination rate.[22] However, adding DCA may not improve the performance of devices having a high-quality film morphology. Tian *et al.* reported the same structure using the **YC-2** dye; however, they did not report the effects of adding DCA coabsorbent on **S1** or **D-2**.[12, 23] In this study, we revealed that adding DCA (10 mM) to **YC-2** (up to 5.36%) and **YC-3** (5.28%) improved the quantum efficiency by 4%–9% (Table 2 and Fig. 8). In the presence of DCA, both of the V_{oc} and J_{sc} values considerably increased, indicating the improvement of film quality and improvement of dye loading in table S4. That indicated the addition a DCA co-absorbent to help dye aligment more vertical on TiO_2 rather than dye lying on the TiO_2 surface. **YC-1** and **YC-4** seem to form a high quality monolayer. Upon adding DCA, both the V_{oc} and FF values remained nearly the same; however, the J_{sc} values decreased from 14.86 to 12.91 mA·cm^{-2} for **YC-1** and from 13.44 to 13.17 mA·cm^{-2} for **YC-4**. Moreover, the quantum efficiency exhibited an overall decrease of 4%–13%. The reduction in the J_{sc} value can be explained by a lower amount of loading because the TiO_2 surface was partly occupied by DCA. The long hexyloxy substituents in **YC-1** and **YC-4** not only cover the TiO_2 surface but also form a high-quality film morphology. This effect is supported by the higher resistance in the electrochemical impedance spectrum (EIS), presented in the following section. The relative photovoltaic efficiency of **YC-1** with E1 was higher than that with the other electrolytes; this difference is attributed to the higher efficiency of electron injection to the conduction band of TiO_2, and it exhibited an IPCE of 60% in the region of 385–605 nm, a J_{sc} value of 14.86 mA·cm^{-2}, a V_{oc} value of 0.67 V, and an FF of 0.62 corresponding to an overall conversion efficiency of 6.18%.

Table 2 Photovoltaic parameters of DSSCs fabricated using **YC-1–4** with and without deoxycholic acid

dye	DCA^{a} (mM)	J_{sc} ($mA{\cdot}cm^{-2}$)	V_{oc} (V)	FF	η^{b} (%)
YC-1	0	14.86	0.67	0.62	6.18
	10	12.91	0.67	0.63	5.40
YC-2	0	12.18	0.64	0.63	4.92
	10	12.83	0.66	0.64	5.36
YC-3	0	12.43	0.65	0.63	5.08
	10	12.56	0.66	0.63	5.28
YC-4	0	13.44	0.66	0.60	5.37
	10	13.17	0.65	0.60	5.17

[a] Concentration of dye is 3 × 10^{-4} M in CH_2Cl_2. [b] Performance of DSSCs measured in a 0.25 cm^2 working area on an FTO (7 Ω/square) substrate under AM 1.5 condition with electrolyte 1 (E1).

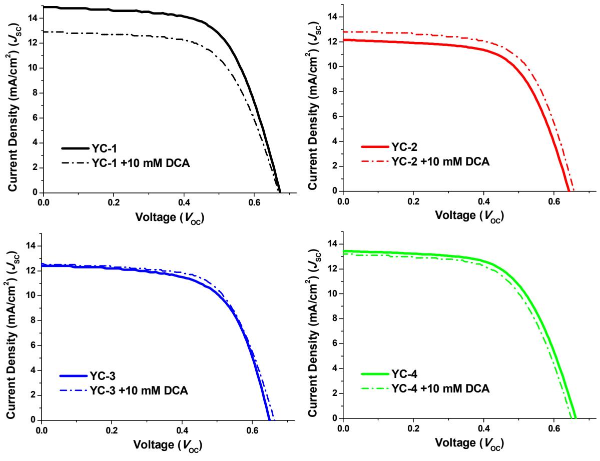

Fig. 8 *J–V* curves of DSSCs fabricated with and without a DCA co-absorbent at a light intensity of 1.0 sun.

View Article Online
DOI: 10.1039/C5RA17898C

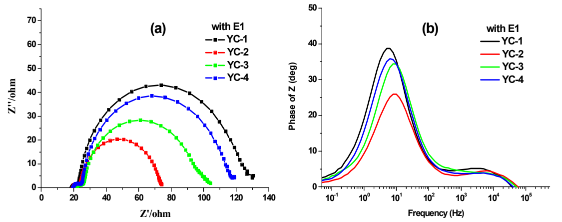

Fig. 9. Impedance spectra of **YC**-series dyes by using E1 electrolyte in CH_2Cl_2 without DCA. **(a)** Nyquist plots (i.e., minus imaginary part of the impedance –Z″ vs. the real part of the impedance Z′ when sweeping the frequency). **(b)** Bode phase plots at -0.70 V bias in the dark.

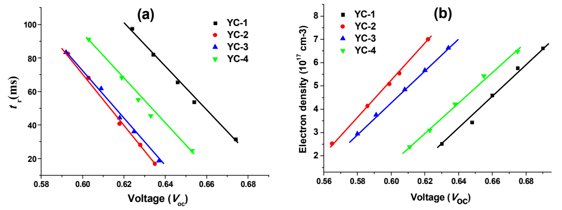

Fig. 10. IMVS and CEM of **YC**-series dyes by using E1 electrolyte in CH_2Cl_2 without DCA. **(a)** Electron lifetime as a function of V_{oc} was measured by IMVS method. **(b)** Electron density as a function of V_{oc} was measured by CEM method.

Electrochemical impedance spectroscopy and life time by CEM / IMVS

EIS analysis was performed to further elucidate the photovoltaic property (Fig. 9). The Nyquist and Bode plots were measured under a forward bias and dark conditions. In the Nyquist plots, a semicircle was observed for each dye; this semicircle is associated with the transport process at the TiO_2/electrolyte/dye interfaces; a larger semicircle corresponds to a larger charge recombination resistance at a low frequency, indicating a lower charge recombination rate and smaller dark current.[24] The radius of the larger semicircles increased in the order **YC-2** < **YC-3** < **YC-4** < **YC-1**, and this trend was consistent with the V_{oc} values in E1. The electron lifetime can be directly estimated by fitting the plots to the equation $\tau = 1/(2\pi f)$ in a Bode plot (Fig. 9b), whereas a shift to a low frequency corresponds to a longer electron lifetime. Furthermore, a larger V_{oc} value of **YC-1** (27.5 ms) and **YC-4** (22.4 ms) corresponds to a longer electron lifetime, and the results revealed that the long hexyloxy chain of the arylamine donor could prevent direct contact between iodine and the TiO_2 surface and reduce the charge recombination rate.

We further verified to measure the electron lifetime (τ_r) by intensity modulated photovoltage spectroscopy (IMVS) method, and displayed in Fig. 10a. The electron lifetime decreases in the order of **YC-1** (31.41 ms) > **YC-4** (24.62 ms) > **YC-3** (18.66 ms) > **YC-2** (16.77 ms) under the same light intensity, the similar trend was also consistent with the data by fitting Bode plots. It's well known, the V_{oc} value is defined as the energy difference between the Fermi level of TiO_2 and the redox couple of the electrolyte.[18] Considering that the redox couple fabricated in the cells is identical (E1 electrolyte), the difference in V_{oc} for **YC-1~4** should be attributed to the electron density in TiO_2. We also performed charge extraction method (CEM) measurement to understand the influence of V_{oc} value with shift in Femi energy level of TiO_2 conduction band. The charge extraction method, as the same the electron density in TiO_2, the conduction band edge of TiO_2 exhibited more up-shift for **YC-1** in Fig. 10b, and this trend was consistent with the Nyquist plots. That high V_{oc} value and electron lifetime were associated balance between electron injection and charge recombination

Conclusions

In summary, we demonstrated that high performance DSSCs can be achieved by using isophorone as the bridge moiety in **YC-1–4** dyes and facilating the dye synthesis route without Pd catalysis. The planar shape of isophorone, with two slightly bulky methyl substituents, exhibited high film-forming ability on the TiO_2 surface. Both **YC-1** and **YC-4** exhibited remarkable solar-to-energy conversion efficiency because they possess favorable light-harvesting capacity and high absorptivity. In the DCA influence experimnet, evidence showed that **YC-1** and **YC-4** sensitisers formed high-quality morphology on TiO_2 without DCA co-absorbent. A typical device fabricated using **YC-1** exhibited an IPCE of 60% in the region of 385–605 nm, a J_{sc} 14.86 mA·cm^{-2}, a V_{oc} of 0.67 V, and an FF of 0.62, corresponding to an overall conversion efficiency of 6.18%. The **YC-1** also displayed higher V_{oc} value and electron lifetime by using impedance/CEM/IMVS method. Although **YC-1** showed the highest performance of 6.18% in this work, still lower than **NKX-2753** and **D-3**. But, we used low cost C-C bond coupling by using a lack of Pd-catalysed procedure for obtaining isophorone derivatives facilitates the preparation of useful dyes for solar cells, and investigated the donor side with long alkyl-chain to simplify device fabrication without addition of DCA.

Acknowledgements

Financial supports from the Ministry of Science and Technology of Taiwan (MOST 103-2113-M-029 -007 -MY2) and Academia Sinica are gratefully acknowledged. Special thanks to Professor C.-P. Hsu at the Institute of Chemistry Sinica of Taiwan for her assistance on quantum chemistry computations.

References

1 M. Grätzel, *Inorg. Chem.*, 2005, **44**, 6841.

2 (*a*) B. O'Regan and M. Grätzel, *Nature*, 1991, **353**, 737. (*b*) Md. K. Nazeeruddin, A. Key, I. Rodicio, R. Humphry-Baker, E. Müller, P. Liska, N. Vlachopoulous and M. Grätzel, *J. Am. Chem. Soc.*, 1993, **115**, 6382. (*c*) M. K. Nazeeruddin, S. M. Zakeeruddin, R. Humphry-Baker, M. Jirousek, P. Liska, N. Vlachopoulous, V. Shklover, C. H. Fischer and M. Grätzel, *Inorg. Chem.*, 1999, **38**, 6298. (*d*) M. K. Nazeeruddin, P. Péchy, T. Renouard, S. M. Zakeeruddin, R. Humphry-Baker, P. Comte, P. Liska, L. Cevey, E. Costa, V. Shklover, L. Spiccia, G. B. Deacon, C. A. Bignozzi and M. Grätzel, *J. Am. Chem. Soc.*, 2001, **123**, 1613. (*e*) P. Wang, S. M. Zakeeruddin, J. E. Moser, M. K. Nazeeruddin, T. Sekiguchi and M. Grätzel, *Nature Materials*, 2003, **2**, 402.

3 A. Yella, H. W. Lee, H. N. Tsao, C. Yi, A. K. Chandiran, M. K. Nazeeruddin, E. W. G. Diau, C. Y. Yeh, S. M. Zakeeruddin and M. Grätzel, *Science*, 2011, **334**, 629.

4 (*a*) Z. S. Wang, Y. Cui, K. Hara, Y. Dan-oh, C. Kasada and A. Shinpo, *Avd. Mater.*, 2007, **19**, 1138. (*b*) D. Kuang, S. Uchida, R. Humphry-Baker, S. M. Zakeeruddin and M. Grätzel, *Angew. Chem., Int. Ed.*, 2008, **47**, 1923. (*c*) H. Choi, C. Baik, S. O. Kang, J. Ko, M.-S. Kang, M. K. Nazeeruddin and M. Grätzel, *Angew. Chem., Int. Ed.*, 2008, **47**, 327. (*d*) S. Ito, H. Miura, S. Uchida, M. Takata, K. Sumioka, P. Liska, P. Comte, P. Péchy and M. Grätzel, *Chem. Commun.*, 2008, 5194. (*e*) H. Qin, S. Wenger, M. Xu, F. Gao, X. Jing, P. Wang, S. M. Zakeeruddin and M. Grätzel, *J. Am. Chem. Soc.*, 2008, **130**, 9202. (*f*) Y. J. Chang and T. J. Chow, *Tetrahedron*,

View Article Online
DOI: 10.1039/C5RA17898C

2009, **65**, 4726. *(g)* H. Tian, X. Yang, J. Cong, R. Chen, J. Liu, Y. Hao, A. Hagfeldt and L. Sun, *Chem. Commun.,* 2009, 6288. (*h*) Y. Wu, M. Marszalek, S. M. Zakeeruddin, Q. Zhang, H. Tian, M. Grätzel and W. Zhu, *Energy Environ. Sci.*, 2012, **5**, 8261. (*i*) N. Cai, R. Li, Y. Wang, M. Zhang and P. Wang, *Energy Environ. Sci.*, 2013, **6**, 139. (*j*) Y. J. Chang, P.-T. Chou, Y.-Z. Lin, M. Watanabe, C.-J. Yang, T.-M. Chin and T. J. Chow, *J. Mater. Chem.*, 2012, **22**, 21704. (*k*) X.-H. Zhang, Z.-S. Wang, Y. Cui, N. Koumura, A. Furube and K. Hara, *J. Phys. Chem. C,* 2009*,* **113**, 13409. (*l*) R. Y.-Y. Kin, H.-W. Lin, Y.-S. Yen, C.-H. Chang, H.-H, Chou, P.-W. Chen, C.-Y. Hsu, Y.-C. Chen, J. T. Lin and K.-C. Ho, *Energy Environ. Sci.*, 2013, **6**, 2477. (*m*) S. Cai, X. Hu, Z. Zhang, J. Su, X. Li, A. Islam, L. Han and H. Tian, *J. Mater. Chem. A*, 2013, **1**, 4763.

5 (*a*) N. Koumura, Z.-S. Wang, S. Mori, M. Miyashita, E. Suzuki and K. Hara, *J. Am. Chem. Soc.*, 2006, **128**, 14256. (*b*) Z.-S. Wang, N. Koumura, Y. Cui, M. Takahashi, H. Sekiguchi, A. Mori, T. Kubo, A. Furube and K. Hara, *Chem. Mater.*, 2008, **20**, 3993.

6 (*a*) J. T. Lin, P.-C. Chen, Y.-S. Yen, C.-Y. Hsu, H.-H, Chou and M.-C. P. Yeh, *Org. Lett.*, 2009, **11**, 97. (*b*) S. Qu, C. Qin, A. Islam, Y. Wu, W. Zhu, J. Hua, H. Tian and L. Han, *Chem. Commun.*, 2012, **48**, 6972.

7 (*a*) H. Li, Y. Hou, Y. Yang, R. Tang, J. Chen, H. Wang, H. Han, T. Peng, Q, Li and Z. Li, *ACS Appl. Mater. Interfaces*, 2013, **5**, 12469. (*b*) H. Li, L. Yang, R. Tang, Y. Hou, Y. Yang, H. Wang, H. Han, J. Qin, Q, Li and Z. Li, *Dyes and Pigments*, 2013, **99**, 863.

8 Y. J. Chang, Y.J. Wu, P.-T. Chou, M. Watanabe and T. J. Chow, *Thin Solid Film*, 2014, **558**, 330.

9 (*a*) S. Qu, W. Wu, J. Hua, C. Kong, Y. Long and H. Tian, *J. Phys. Chem. C*, 2010, **114**, 1343. (*b*) S. Qu, B. Wang, F. Guo, J. Li, W. Wu, C. Kong, Y. Long and J. Hua, *Dyes and Pigments,* 2012, **92**, 1384. (*c*) T. W. Holcombe, J.-H. Yum, Y. Kim, K. Rakstys and M. Grätzel, *J. Mater. Chem. A*, 2013, **1**, 13978.

10 (*a*) M. Velusamy, K. R. Justin Thomas, J. T. Lin, Y.-C. Hsu and K.-C. Ho, *Org. Lett.*, 2005, **7**, 1899. (*b*) W. Zhu , Y. Wu , S. Wang , W. Li , X. Li , J. Chen, Z.-S. Wang, and H. Tian, *Adv. Funct. Mater.*, 2011, **21**, 756. (*c*) S. Haid, M. Marszalek, A. Mishra, M. Wielopolski, J. Teuscher, J.-E. Moser, R. Humphry-Baker, S. M. Zakeeruddin, M. Grätzel and P. Bäuerle, *Adv. Funct. Mater.*, 2012, **22**, 1291. (*d*) S. Qu, W. Wu, J. Hua, C. Kong, Y. Long and H. Tian, *J. Phys. Chem. C*, 2010, **114**, 1343.

11 Z.-S. Wang, K. Hara, Y. Dan-oh, C. Kasada, A. Shinpo, S. Suga, H. Arakawa and H. Sugihara, *J. Phys. Chem. B*, 2005, **109**, 3907.

12 B. Liu, W. Zhu, Q. Zhang, W. Wu, M. Xu, Z. Ning, Y. Xie and H. Tian, *Chem. Commun.*, 2009, 1766.

13 C.-J. Yang, Y. J. Chang, M. Watanabe, Y.-S. Hon and T. J. Chow, *J. Mater. Chem.*, 2012, **22**, 4040.

14 (*a*) M. Akhtaruzzaman, Y. Seya, N. Asao, A. Islam, E. Kwon, El-Shafei, L. Han and Y. Yamamoto, *J. Mater. Chem.*, 2012, **22**, 10771. (*b*) W. Li, Y. Wu, X. Li, Y. Xie and W. Zhu, *Energy Environ. Sci.*, 2011, **4**, 1830.

15 (*a*) T. Kitamura, M. Ikeda, K. Shigaki, T. Inoue, N. A. Anderson, X. Ai, T. Lian and S. Yanagida, *Chem. Mater.*, 2004, **16**, 1806. (*b*) S. L. Li, K. J. Jiang, K. F. Shao and L. M. Yang, *Chem. Commun.*, 2006, 2792. (*c*) S. Kim, H. Choi, D. Kim, K. Song, S. O. Kang and J. Ko, *Tetradron.*, 2007, **63**, 9206. (*d*) K. Hara, Z. S. Wang, T. Sato, A. Furube, R. Katoh, H. Sugihara, Y. Dan-oh, C. Kasada, A. Shinpo and S. Suga, *J. Phys. Chem. B.*, 2005, **109**, 15476. (*e*) D. P. Hagberg, T. Edvinsson, T. Marinado, G. Boschloo, A. Hagfeldt and L. Sun, *Chem. Commun.*, 2006, 2245.

16 Y. Shao, L. F. Molnar, Y. Jung, J. Kussmann, C. Ochsenfeld, S. T. Brown, A. T. B. Gilbert, L. V. Slipchenko, S. V. Levchenko, D. P. ONeill, R. A. Jr. DiStasio, R. C. Lochan, T. Wang, G. J. O. Beran, N. A. Besley, J. M. Herbert, C. Y. Lin, T. V. Voorhis, S. H. Chien, A. Sodt, R. P. Steele, V. A. Rassolov, P. E. Maslen, P. P. Korambath, R. D. Adamson, B. Austin, J. Baker, E. F. C. Byrd, H. Dachsel, R. J. Doerksen, A. Dreuw, B. D. Dunietz, A. D. Dutoi, T. R. Furlani, S. R. Gwaltney, A. Heyden, S. Hirata, C.-P. Hsu, G. Kedziora, R. Z. Khalliulin, P. Klunzinger, A. M. Lee, M. S. Lee, W. Z. Liang, I. Lotan, N. Nair, B. Peters, E. I. Proynov, P. A. Pieniazek, Y. M. Rhee, J. Ritchie, E. Rosta, C. D. Sherrill, A. C. Simmonett, J. E. Subotnik, H. L., III Woodcock, W. Zhang, A. T. Bell and A. K. Chakraborty, *Phys. Chem. Chem. Phys.* 2006, **8**, 3172.

17 (*a*) Y. J. Chang, M. Watanabe, P.-T. Chou and T. J. Chow, *Chem. Commun.,* 2012, **48**, 726. (*b*) C. H. Huang and Y. J. Chang, *Tetrahedron Lett.*, 2014, **55**, 4938.

18 (*a*) H. Tian, X. Yang, R. Chen, R. Zhang, A. Hagfeldt and L. Sun, *J. Phys. Chem. C*, 2008, **112**, 11203. (*b*) R. Chen, G. Zhao, X. Yang, X. Jiang, J. Liu, H. Tian, Y. Gao, X. Liu, K. Han, M. Sun and L. Sun, *J. Mol. Struct.,* 2008, **876**, 102.

19 (*a*) G. Boschloo, L. Häggman and A. Hagfeldt, *J. Phys. Chem. B* 2006, **110**, 13144. (*b*) Z. Ning, Y. Fu and H. Tian, *Energy Environ. Sci.,* 2010, **3**, 1170. (*c*) S. A. Haque, E. Palomares, B. M. Cho, A. N. M. Green, N. Hirita, D. R. Klug and J. R. Durrant, *J. Am. Chem. Soc.* 2005, **127**, 3456.

20 M. K. Nazeeruddin, F. D. Angelis, S. Fantacci, A. Selloni, G. Viscardi, P. Liska, S. Ito, B.Takeru and M. Grätzel, *J. Am. Chem. Soc.*, 2005, **127**, 16835.

21 (*a*) J. E. Kroeze, N. Hirata, S. Koops, M. K. Nazeeruddin, L. Schmidt-Mende, M. Grätzel and J. R. Durrant, *J. Am. Chem. Soc.* 2006, **128**, 16376. (*b*) C. Kim, H. Choi, S. Kim, C. Baik, K. Song, M.-S. Kang, S. O. Kang and J. Ko, *J. Org. Chem.*, 2008, **73**, 7072. (*c*) Z. Ning, Q. Zhang, H. Pei, J. Luan, C. Lu, Y. Cui and H. Tian, *J. Phys. Chem. C*, 2009, **113***,* 10307.

22 (*a*) J. Bisquert, *J. Phys. Chem. B*, 2002, **106**, 325. (*b*) Q. Wang, J. Moser and M. Grätzel, *J. Phys. Chem. B*, 2005, **109**, 14945. (*c*) R. Kern, R. Sastrawan, J. Ferber, R. Stangl and J. Luther, *Electrochim. Acta* 2002, **47**, 4213.

23 Z. Ning, Q. Zhang, W. Wu, H. Pei, B. Liu and H. Tian, *J. Org. Chem.*, 2008, **73**, 3971.

24 (*a*) D. Kim, M. S.Kang, K. Song, S. O. Kang and J. Ko, *Tetrahedron*, 2008, **64**, 10417. (*b*) N. Cho, H. Choi, D. Kim, K. Song, M. S. Kang, S. O. Kang and J. Ko, *Tetrahedron*, 2009, **65**, 6236.